

Vulnerability Detection with Graph Simplification and Enhanced Graph Representation Learning

Xin-Cheng Wen^{1*}, Yupan Chen^{1*}, Cuiyun Gao^{1*}, Hongyu Zhang², Jie M. Zhang³, Qing Liao^{1◦}

¹ School of Computer Science and Technology, Harbin Institute of Technology, Shenzhen, China

² School of Big Data and Software Engineering, Chongqing University, China

³ Department of Informatics, King's College London, UK

xiamenwxc@foxmail.com, cyp36889@gmail.com, gaocuiyun@hit.edu.cn,

hyzhang@cqu.edu.cn, jie.zhang@kcl.ac.uk, liaoqing@hit.edu.cn

Abstract—Prior studies have demonstrated the effectiveness of Deep Learning (DL) in automated software vulnerability detection. Graph Neural Networks (GNNs) have proven effective in learning the graph representations of source code and are commonly adopted by existing DL-based vulnerability detection methods. However, the existing methods are still limited by the fact that GNNs are essentially difficult to handle the connections between long-distance nodes in a code structure graph. Besides, they do not well exploit the multiple types of edges in a code structure graph (such as edges representing data flow and control flow). Consequently, despite achieving state-of-the-art performance, the existing GNN-based methods tend to fail to capture global information (*i.e.*, long-range dependencies among nodes) of code graphs.

To mitigate these issues, in this paper, we propose a novel vulnerability detection framework with grAph siMplification and enhanced graph rePrEsentation LEarning, named AMPLE. AMPLE mainly contains two parts: 1) graph simplification, which aims at reducing the distances between nodes by shrinking the node sizes of code structure graphs; 2) enhanced graph representation learning, which involves one edge-aware graph convolutional network module for fusing heterogeneous edge information into node representations and one kernel-scaled representation module for well capturing the relations between distant graph nodes. Experiments on three public benchmark datasets show that AMPLE outperforms the state-of-the-art methods by 0.39%-35.32% and 7.64%-199.81% with respect to the accuracy and F1 score metrics, respectively. The results demonstrate the effectiveness of AMPLE in learning global information of code graphs for vulnerability detection.

Index Terms—Software vulnerability, graph simplification, graph representation learning

I. INTRODUCTION

Software vulnerabilities are weaknesses in source code that can be exploited to cause safety issues such as user information leakage [1] and cyber extortion [2]. The number of disclosed vulnerabilities constantly increases, causing more and more significant concerns in the field of software industry and cybersecurity. For example, the National Vulnerability

Database (NVD) in the US [3] released 8,051 vulnerabilities in the first quarter of 2022, with an increase of 25% over the same period last year [4]. Most recently, Synopsys Open Source Security and Risk Analysis (OSSRA) analyzed 2,409 codebases and found that 81% of them contained at least one known open source vulnerability [5]. The severity and prevalence of software vulnerabilities make it critical to develop accurate automatic vulnerability detection techniques.

Conventional vulnerability detection methods [6]–[10] mainly adopt pre-defined rules provided by human experts to conduct code analysis, which are labor intensive and inaccurate. Recently, many Deep Learning (DL)-based vulnerability detection methods have been proposed [11]–[15], which achieve state-of-the-art performance in vulnerability detection via automatically learning the patterns of vulnerable code without human heuristics. The DL-based methods [11]–[14] generally leverage the structural information of source code and represent code as a *code structure graph* such as Control Flow Graph (CFG), Data Flow Graph (DFG), and Code Property Graph (CPG) [16]. The information in these graphs can also be integrated with Abstract Syntax Tree (AST) and Natural Code Sequence (NCS) to provide more comprehensive graph representations [17].

Code structure graphs typically contain complex hierarchical information [18], [19]. To effectively learn the representations of code structure graphs, state-of-the-art DL-based methods utilize a variety of Graph Neural Network (GNN) models such as Gated Graph Neural Network (GGNN) [20] and Graph Convolution Network (GCN) [21]. However, it is well acknowledged that GNN models have limitations in handling long-distance connections between nodes that are not directly adjacent to each other [22], [23]. Although one can use GNNs with stacked multiple layers to learn global information (*i.e.*, long-range dependencies among nodes) of the graph, the over-smoothing issue [24], [25] yielded from a deep GNN will lead to similar embeddings for nodes with different labels, thereby degrading the overall performance [26]. Moreover, the code structure graphs typically contain multiple types of relations (*e.g.*, edges representing data flow and control flow) [20], [21]. The existing GNN models (*e.g.* GGNN, GCN [27]) cannot adequately model the edge features in a graph [28],

* These authors contribute to the work equally and are co-first authors of the paper.

* Corresponding author. The author is also affiliated with Peng Cheng Laboratory and Guangdong Provincial Key Laboratory of Novel Security Intelligence Technologies.

◦ The author is also affiliated with Peng Cheng Laboratory.

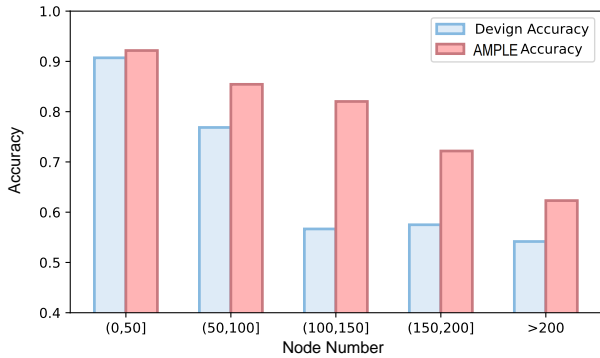


Fig. 1: Accuracy of Devign [17] and AMPLE on the Reveal dataset [20] with different numbers of graph nodes.

which further limits their capability to capture global information of a code structure graph. Therefore, despite achieving state-of-the-art performance, existing DL-based models still have difficulties in capturing the global information of source code, which hinders their performance in detecting software vulnerabilities especially for complex graphs.

Taking Devign [17], a recent GNN-based vulnerability detection model as an example, we analyze the relationship between model performance and the number of graph nodes. Devign learns vulnerable code patterns from code structure graphs that contain four types of edges (AST, CFG, DFG, and NCS). We experiment on the Reveal dataset [20]. The data in the test set are divided into five intervals based on the number of nodes in code structure graphs, with results shown in Figure 1. As can be seen, Devign shows obviously better performance for the graphs with fewer nodes, *e.g.*, achieving 90% accuracy for graphs with no more than 50 nodes, and drops severely as the number of nodes increases. For the graphs with more than 200 nodes, the accuracy of Devign is only around 54%. The results indicate the ineffectiveness of current methods in learning global code information.

In this paper, we propose **AMPLE**, a novel vulnerability detection framework with **grAph siMplification** and **enhanced graph rePResentation LEarning**. AMPLE contains two major parts: 1) **Graph simplification**, which reduces the distances between nodes by shrinking the sizes of code structure graphs. 2) **Enhance graph representation learning**, which includes two modules. The edge-aware graph neural network module considers the information of edge types and fuses the heterogeneous edge information into node representations; while the kernel-scaled representation module scales up the convolution kernel size for explicitly capturing the relationship between distant graph nodes.

To evaluate AMPLE, we use three widely-studied benchmark datasets in software vulnerability detection: FFM-Peg+Qemu [17], Reveal [20], and Fan et al. [29]. We compare AMPLE with six existing software vulnerability detection methods, including three state-of-the-art graph-based and three token-based methods. The results demonstrate that AMPLE outperforms all the baseline methods with respect to the

accuracy and F1 score metrics. In particular, AMPLE achieves 4.75%, 6.86%, and 9.24% absolute improvement in F1 score over the state-of-the-art on the three datasets, respectively, with the corresponding relative improvements at 7.63%, 16.48%, and 40.40%.

In summary, the major contributions of this paper are as follows:

- 1) We propose AMPLE, a novel vulnerability detection framework. AMPLE involves a new code input representation for reducing the distances between nodes and an enhanced graph representation learning method for better capturing the information code structure graphs.
- 2) We perform a large-scale evaluation of AMPLE on three public benchmark datasets, and the results demonstrate the effectiveness of AMPLE in accurate vulnerability detection.

The remaining of this paper is organized as follows. Section II introduces the background and related work. Section III presents the overall architecture of AMPLE and the two parts in detail, including graph simplification and enhanced graph representation learning. Section IV describes the experimental setup, including datasets, baselines and experimental settings. Section V introduces the experimental results and analysis. Section VI discusses why AMPLE can effectively detect code vulnerability and the threats to validity. Section VII concludes this paper.

II. BACKGROUND AND RELATED WORK

In this section, we introduce the background and related work about vulnerability detection, from the perspectives of the code representation and deep learning models.

A. Code Representation in Vulnerability Detection

Early DL-based vulnerability detection methods [11], [12], [14], [32], [33] regard source code as flat sequences and adopt natural language processing techniques for representing the input code. They generally initialize the embeddings of tokens with word2vec [34]. Despite that these methods do not require code integrity and syntax correctness, they neglect the inherent structural regularity of code, and may only focus on shallow semantics [17]. To well exploit the structural information of code, a series of methods [13], [15], [20], [21], [35]–[39] abstract the code in the form of graphs (*e.g.* AST, CFG, DFG, PDG) and use the graphs as the model input. Following the work of Devign [17], we construct a comprehensive code structure graph, which is treated as a heterogeneous graph to obtain the semantic and syntactic information represented by different edge types. We further simplify the code structure graph to shrink the graph size and boost the model to learn the global representation.

B. Deep-learning Models for Vulnerability Detection

The neural networks used in early work include Convolutional Neural Network (CNN) [40], [41] and Recurrent Neural Network (RNN) [42], [43]. For example, Russell *et al.* [12] input the lexical code representation into CNN. Vuldeepecker

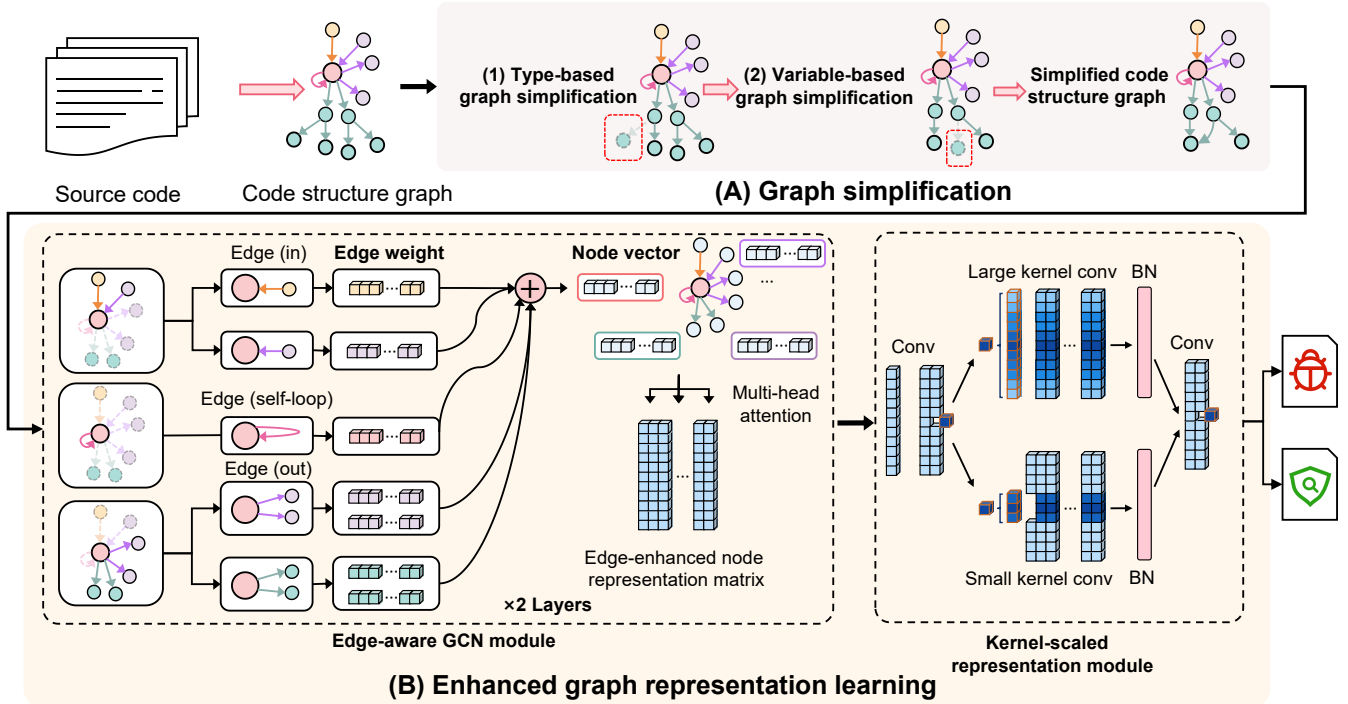


Fig. 2: Architecture of AMPLE, which mainly contains two parts: (A) graph simplification and (B) enhanced graph representation learning. Nodes with different colors in the simplified code structure graph indicate their edge types are different, e.g., edges of CFG or DFG. Conv [30] represents convolutional layer. BN [31] is the batch normalization layer.

[11] employs BiLSTM to handle the code gadgets, a fine-grained code slice. Some work [13], [44] also selects LSTM as code encoders. Recently, GNN-based methods [17], [20], [21] have achieved state-of-the-art performance on vulnerability detection. GNN [45], [46] is a type of neural network which directly operates on graph structure. Devign [17] and Reveal [20] adopt GGNN [47] to process multiple directed graphs generated from source code. However, GGNN converts different edge types into an adjacency matrix without distinguishing them, leading to limited performance as the number of edge types increases [48]. IVDetect [21] leverages Graph Convolutional Network (GCN) and uses a context vector to predict vulnerabilities. However, GCN focuses on learning the local features of nodes by neighborhood aggregation, and thereby tends to fail to capture long-range dependencies among nodes as the graph sizes increase [49]. In this work, we aim at mitigating the issues of GNNs for better learning the global information of code structure graphs in vulnerability detection.

III. AMPLE FRAMEWORK

In this section, we introduce the detailed architecture of AMPLE. As shown in Figure 2, AMPLE mainly consists of two parts: (A) Graph simplification (*c.f.*, Section III-A), which condenses the repetitive information in code structure graph through type-based graph simplification and variable-based graph simplification; (B) Enhanced graph representation learning, which contains the edge-aware graph convolutional

network module (*c.f.*, Section III-B1) to learn edge-enhanced node representations and the kernel-scaled representation module (*c.f.*, Section III-B2) to capture the relations between distant graph nodes.

TABLE I: Merging rules in type-based graph simplification. “PType” and “CType” indicate the types of the parent and child nodes of a directed edge, respectively. The * represents any node type, and the PType “Augment” in Rule 6 represents the parameters of function call statements.

Rule	PType	CType
1	ExpressionStatement	AssignmentExpression UnaryExpression CallExpression PostIncDecOperationExpression
2	IdentifierDeclStatement	IdentifierDecl
3	Condition	*
4	ForInit	*
5	CallExpression	ArgumentList
6	Argument	*
7	Callee	Identifier

A. Graph Simplification

The graph simplification part aims at condensing the repetitive information in a code structure graph, which can shrink graph sizes and reduce the distances between nodes. We propose two simplification steps: type-based graph simplification (according to node types) followed by variable-based graph

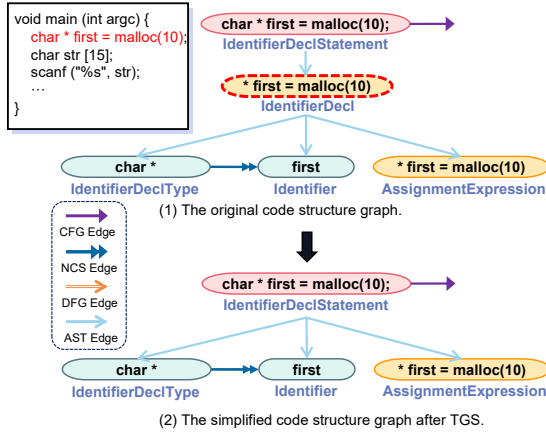


Fig. 3: An example illustrating type-based graph simplification. The text in/under each node represents the node value/type. Some nodes and edges are omitted for facilitating illustration. The node with red dashed border in the original code structure graph (1) is merged with its parent node, producing a TGS-based simplified graph (2).

simplification (according to node variables). In the following, we first elaborate on the two steps, and then provide an algorithm of the overall process.

1) *Type-based Graph Simplification*: The type-based graph simplification (TGS) method aims at merging adjacent nodes according to the node types. According to the parsing principles [50] and manually examining the code structure graphs, we have identified seven merging rules for type-based graph simplification. Table I lists the summarized merged rules, where $PType$ and $CType$ denote the type of the parent node and child node, respectively. The merging rule 1, 2, 3, 4 and 5-7 correspond to different types of statements including expression statement, identifier declaration statement, condition statement, for-loop statement and function call statement, respectively, in the studied C/C++ programming language. For each pair of adjacent nodes matching one merging rule, the child node will be removed since its information is the refinement of its parent node and can also be reflected in its subsequent nodes. Figure 3 illustrates an example of the TGS-based simplification process. In Figure 3 (1), the node with red dashed border is merged to its parent node according to Rule 2 in Table I. Specifically, the information in the child node “* first = malloc(10)” is also covered by the parent node and its three child nodes. Due to the page limit, we illustrate the simplification based on other rules in the published repository¹.

2) *Variable-based Graph Simplification*: The variable-based graph simplification (VGS) method aims at merging leaf nodes according to the node variables. Specifically, the VGS method merges the nodes with repeated variables into one node in the code structure graph. It only applies to the leaf nodes

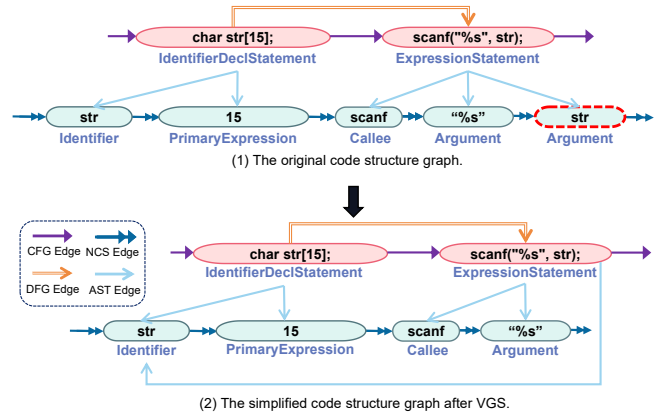


Fig. 4: An example illustrating variable-based graph simplification. The node with red dashed border in the original code structure graph (1) is merged to the previous node “str”, producing a VGS-based simplified code structure graph (2).

of AST and does not change the hierarchical parent-child information [51]. Besides, since the merged variable node has more than one parent node, it can aggregate information from different statements simultaneously. This can enhance the node representations and facilitate the global graph representation learning. Figure 4 presents an example of variable-based graph simplification. The variable “str” appears in the child nodes of both “char str[15]; ” and “scanf(“%s”,str);”, thereby we merge the two “str” leaf nodes.

3) *The Algorithm of Graph Simplification*: The overall graph simplification (GS) process is depicted in Algorithm 1, in which TGS and VGS correspond to Lines 2-19 and Lines 20-25, respectively. The algorithm takes the original code structure graph as the input, and outputs the simplified code structure graph based on TGS and VGS. For TGS, the algorithm performs breadth-first traversal on AST. Each time encountering a pair of adjacent nodes (u, v) conforming to the merging rules in Table I (Line 10), the following operations are performed (Lines 11-12): deleting v and the edges connected with v , and then adding new edges between u and all the child nodes of v . For VGS, the algorithm first obtains all groups containing the same variable, and then merges the nodes with same variable into one node. The final simplified code structure graph is fed into the subsequent part of AMPLE.

B. Enhanced Graph Representation Learning

To enhance graph representation learning, we design two modules: the **edge-aware graph convolutional network module** for fusing heterogeneous edge information into node representations, and the **kernel-scaled representation module** which scales up the convolutional kernel size to capture the relations between distant nodes in the graph.

1) *Edge-Aware Graph Convolutional Network Module*: The edge-aware graph convolutional network (EA-GCN), as shown in the left of Figure 2 (B), is proposed to exploit different edge types, e.g., AST and CFG, in the directed simplified

¹<https://github.com/AMPLE001/AMPLE>

Algorithm 1: Graph simplification

Input : Original Code Structure Graph: $Graph_{Original}$
Output: Simplified Code Structure Graph: $Graph_{GS}$

```

1 Function GS:
  // The procedure of TGS
2  $Graph_{TGS} \leftarrow Graph_{Original}$ 
3 for each AST  $T \in Graph_{TGS}$  do
  // Do breadth-first traversal
4  $Stack \leftarrow \emptyset$ 
5 Pushing  $T.root$  into  $Stack$ 
6 while  $Stack \neq \emptyset$  do
7    $u \leftarrow Pop\ Stack$ 
8    $Children \leftarrow$  Get all the child nodes of  $u$ 
9   for  $v \in Children$  do
10    if  $(u.Type, v.Type)$  conform to rules in Table 1
11     then
12      Delete edge  $(u, v)$  and  $v$  from  $Graph_{TGS}$ ;
13      Add edges between  $u$  and all child nodes of
14       $v$ ;
15      Push all child nodes of  $v$  into  $Stack$ ;
16     else
17      Push  $v$  into  $Stack$ ;
18     end
19   end
20 end
  // The procedure of VGS
21  $Graph_{GS} \leftarrow Graph_{TGS}$ 
22  $leaf\_nodes \leftarrow$  get all the leaf nodes of AST in  $Graph_{GS}$ 
23  $same\_variable \leftarrow$  get all the node groups with the same
24   variable in  $leaf\_nodes$ 
25 for each  $group \in same\_variable$  do
26   | Merging all the nodes in the  $group$  into one variable node
27 end
28 return  $Graph_{GS}$ 

```

graph for enhancing node representations. EA-GCN module first computes node vectors by weighting edges of different types separately, and then enhances node representations based on multi-head attention.

We denote the input simplified code structure graph as $G(\mathcal{V}, \mathcal{E}, \mathcal{R})$. \mathcal{V} is the set of nodes in the graph and each node $v_i \in \mathcal{V}$ is initialized as $h_i^0 \in \mathbb{R}^d$ by word2vec [34], where d is the vector dimension. \mathcal{E} represents the set of edges and $(v_i, \beta, v_j) \in \mathcal{E}$ denotes a labeled edge, where $\beta \in \mathcal{R}$ indicates the edge type and \mathcal{R} is the set of edge types.

During the message passing, we propose to incorporate multiple edge information into node embeddings. Specifically, for node v_i with edge type β in the graph, we compute the edge weight W_β^l in the l -th layer as:

$$W_\beta^l = a_\beta^l V^l, \quad (1)$$

where a_β^l is a learnable weight specific to the edge type β , and $V^l \in \mathbb{R}^{d \times d}$ represents a linear transformation. We then employ the edge weight to update the representation of the node v_i based on the following propagation mechanism:

$$h_i^l = \sigma \left(\sum_{\beta \in \mathcal{E}} \sum_{j \in N_i^\beta} \frac{1}{c_{i,\beta}} W_\beta^l h_j^{l-1} + W_0^l h_i^{l-1} \right), \quad (2)$$

where h_i^l is the hidden state of node v_i , N_i^β denotes the set of indices of neighborhood nodes with the edge type β , and $c_{i,\beta}$ is the number of neighboring nodes.

To further exploit the heterogeneous edge information in the graph, we propose to adopt multi-head attention mechanism [52]. The attention mechanism is capable of controlling how much different edge information contributes to the node representation. The attention score $w_{i \rightarrow j}^{k,l}$ for the edge from source node v_i to destination node v_j is computed as below.

$$w_{i \rightarrow j}^{k,l} = \text{softmax}_j \left(\frac{h_i^{k,l} \cdot h_j^{k,l}}{\sqrt{d_k}} \right), \quad (3)$$

where k denotes the attention head number, and $h_i^{k,l}$ and $h_j^{k,l}$ denote the representations of v_i and v_j , respectively. The node representation h_i^l is enhanced by aggregating the attention scores of the node edges:

$$A_i^l = \text{Concat}_{k=1}^P \left(\sum_{j \in N_i} w_{i \rightarrow j}^{k,l} h_j^{k,l} \right) W_h^l + h_i^{l-1}, \quad (4)$$

$$h_i^l = W_2^l \cdot \sigma \left(W_1^l A_i^l \right) + A_i^l, \quad (5)$$

where N_i denotes the set of neighboring nodes of the node v_i and P is the number of attention heads. The $\text{Concat}(\cdot)$ denotes the combination of representations of different heads, and $\sigma(\cdot)$ is the activation function. W_1^l and W_2^l are linear transformation layers with bias terms. We finally compute the edge-enhanced node representation matrix of the whole graph as $H_i^l = \{h_k^l\}_{k=1}^{|\mathcal{V}|}$. $|\mathcal{V}|$ denotes the number of nodes in the graph.

2) *Kernel-scaled Representation Module*: The module aims at learning the global information of graphs by explicitly capturing the relations between distant nodes. Specifically, the kernel-scaled representation module involves two convolution kernels with different scales, *i.e.*, one with a large kernel and the other with a small kernel. The large kernel and small kernel are designed to focus on the relations between distant nodes and neighborhood nodes, respectively.

Given the edge-enhanced node representation matrix H_i^l , the module conducts kernel-scaled convolution, in which the large and small kernel sizes are denoted as N and M ($M < N$), respectively. The convolution with different kernel scales is conducted in parallel, and the output based on the double-branch convolution is defined as:

$$K^{out} = \text{BN} \left(H_i^l * W^L, \mu^L \right) + \text{BN} \left(H_i^l * W^S, \mu^S \right), \quad (6)$$

where $*$ is the convolution operator. $W^L \in \mathbb{R}^{C_{out} \times C_{in} \times N}$ and $W^S \in \mathbb{R}^{C_{out} \times C_{in} \times M}$ denote the large convolution kernel and small convolution kernel, respectively, where C_{in} and C_{out} are the input and output channels of the convolution. The results of the two branches are summed after passing through a batch normalization (BN) layer [31]. μ^L is the parameter of the BN layer following the large convolution kernel and μ^S is for the other branch. Finally, we use two fully-connected (FC)

TABLE II: Statistics of the datasets.

Dataset	Samples	Vul	Non-vul	Vul Ratio(%)
FFMPeg+Qemu [17]	22,361	10,067	12,294	45.02
Reveal [20]	18,169	1,664	16,505	9.16
Fan <i>et al.</i> [29]	179,299	10,547	168,752	5.88

layers and a softmax function to perform binary classification (vulnerable or non-vulnerable).

IV. EXPERIMENTAL SETUP

A. Research Questions

In order to evaluate AMPLE, we answer the following research questions:

- RQ1:** How effective is AMPLE in vulnerability detection?
- RQ2:** How does graph simplification contribute to the performance of AMPLE?
- RQ3:** How does enhanced graph representation learning contribute to the performance of AMPLE?
- RQ4:** What is the influence of hyper-parameters on the performance of AMPLE?

B. Datasets

To investigate the effectiveness of AMPLE, following IVDetect [21], we adopt three vulnerability datasets in our study, including FFMPeg+Qemu [17], Reveal [20], and Fan *et al.* [29]. The statistics of the experimental datasets are illustrated in Table II. The FFMPeg+Qemu dataset provided by Devign [17] is manually-labeled and comes from two open-source C projects. It contains about 10k vulnerable entries and 12k non-vulnerable entries. The Reveal dataset [20] is collected from two open-source projects: Linux Debian Kernel and Chromium. It consists of about 2k vulnerable entries and 20k non-vulnerable entries. Fan *et al.* [29] collected from over 300 open-source C/C++ GitHub projects, which cover 91 different vulnerability types from 2002 to 2019 in the Common Vulnerabilities and Exposures (CVE) database. The dataset consists of approximately 10k vulnerable entries and 177k non-vulnerable entries.

C. Baseline Methods

In our evaluation, we compare AMPLE with three state-of-the-art graph-based methods [17], [20], [21] and three token-based methods [11]–[13].

(1) **Devign** [17]: Devign builds a joint graph containing AST, CFG, DFG and NCS, and uses GGNN for vulnerability detection.

(2) **Reveal** [20]: Reveal divides code vulnerability detection into two phases: feature extraction and training. It leverages GGNN to extract features.

(3) **IVDetect** [21]: IVDetect constructs PDG and utilizes GCN to learn the graph representation for vulnerability detection.

(4) **VulDeePecker** [11]: VulDeePecker embeds source code and the data/control dependencies in a program slice through word2vec. It then feeds the embedding into a bidirectional

LSTM-based neural network with an attention mechanism for vulnerability detection.

(5) **Russell *et al.*** [12]: Russell *et al.* label the source code and embed it into the corresponding matrix. They adopt convolutional neural networks, integrated learning, and random forest classifier for code vulnerability detection.

(6) **SySeVR** [13]: SySeVR uses code statements, program dependencies, and program slicing as features, and utilizes a bidirectional recurrent neural network to detect vulnerable code snippets.

D. Implementation Details

To ensure the fairness of the experiments, we use the same data splitting for all approaches. We randomly partition the dataset into disjoint training, validation, and test sets with the ratio of 8:1:1. We reproduce all the baseline models except Devign based on the publicly released source code and use the same hyperparameter settings as described in their original paper. Since Devign itself does not provide the source code, we reproduce the baseline based on the implementation provided by Reveal [20].

Following the work [20], we create the code structure graph based on the results parsed by Joern [50]. The preprocessing steps used to initialize the embedding vectors of each node are as follows: (1) we first tokenize the code in this node as a token sequence, with punctuations kept (2) we initialize the embedding of each token through word2vec [34], without removal of any tokens (3) we compute the average of the token embeddings as the initial embedding of this node. In the embedding layer, the dimension of the initial node representation d_k is set as 100. We adopt RAdam [53] optimizer with a learning rate at 0.0001. The batch size is set to 64. The large kernel M and small kernel N are set to 11 and 3 respectively. The number of EA-GCN layers is 2 and the number of the attention head P is 10. We train our model for a maximum of 100 epochs on a server with NVIDIA GeForce RTX 3090 with 20-epoch patience for early stopping.

E. Performance Metrics

We use the following four widely-used performance metrics in our evaluation:

Precision: $Precision = \frac{TP}{TP+FP}$. Precision is the proportion of relevant instances among those retrieved. TP the number of true positives and FP the number of false positives.

Recall: $Recall = \frac{TP}{TP+FN}$. Recall is the proportion of relevant instances retrieved. TP the number of true positives and FN is the number of false negatives.

F1 score: $F1\ score = 2 \times \frac{Precision \times Recall}{Precision + Recall}$. F1 score is the geometric mean of precision and recall and indicates balance between them.

Accuracy: $Accuracy = \frac{TP+TN}{TP+TN+FN+FP}$. Accuracy is the proportion of correctly classified instances to all instances. TN is the number of true negatives and $TP + TN + FN + FP$ represents the number of all samples.

TABLE III: Comparison results between AMPLE and the baselines on the three datasets. “-” means that the baseline does not apply to the dataset in this scenario. The best result for each metric is highlighted in bold. The cells in grey represent the performance of the top-3 best methods in each metric, with darker colors representing better performance.

Metrics(%) \ Dataset	FFMPeg+Qemu [17]				Reveal [20]				Fan <i>et al.</i> [29]			
	Accuracy	Precision	Recall	F1 score	Accuracy	Precision	Recall	F1 score	Accuracy	Precision	Recall	F1 score
Baseline												
VulDeePecker	49.61	46.05	32.55	38.14	76.37	21.13	13.10	16.17	81.19	38.44	12.75	19.15
Russell <i>et al.</i>	57.60	54.76	40.72	46.71	68.51	16.21	52.68	24.79	86.85	14.86	26.97	19.17
SySeVR	47.85	46.06	58.81	51.66	74.33	40.07	24.94	30.74	90.10	30.91	14.08	19.34
Devign	56.89	52.50	64.67	57.95	87.49	31.55	36.65	33.91	92.78	30.61	15.96	20.98
Reveal	61.07	55.50	70.70	62.19	81.77	31.55	61.14	41.62	87.14	17.22	34.04	22.87
IVDetect	57.26	52.37	57.55	54.84	-	-	-	-	-	-	-	-
AMPLE	62.16	55.64	83.99	66.94	92.71	51.06	46.15	48.48	93.14	29.98	34.58	32.11

V. RESULTS

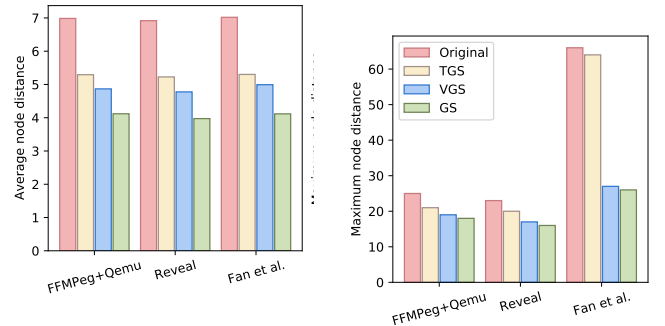
A. RQ1. Effectiveness of AMPLE

To answer the first question, we compare AMPLE with the six baseline methods on the three datasets. The results are illustrated in Table III. Based on the results, we achieve the following observations.

Graph-based methods perform better than token-based methods: We observe that the three graph-based methods Devign, Reveal and IVDetect show superior performance than the three token-based methods in terms of accuracy and F1 score. For example, the cells with grey colors which indicate the top-3 best methods generally appear in the bottom rows of the table. The results demonstrate that graph-based methods can better capture the code structural information, which is beneficial for improving the performance of code vulnerability detection.

The proposed methods consistently outperform all the baseline methods: We observe that AMPLE outperforms all the baseline methods on the three datasets in terms of accuracy and F1 score. Specifically, AMPLE achieves 4.75%, 6.86%, and 9.24% absolute improvement in F1 score over the best baseline method on the three datasets, respectively. The corresponding relative improvements are 7.63%, 16.48%, and 40.40%. When considering all the four performance metrics regarding the three datasets (12 combination cases altogether), AMPLE has the best performance in 10 out of the 12 cases, and top-3 performance in 11 out of the 12 cases. We also make an additional comparison with LineVul [49] on the FFMPeg+Qemu and Reveal datasets. On these two datasets, LineVul achieves the F1-score of 56.54% and 44.79%, respectively; while our proposed model achieves 66.94% and 48.48%, respectively.

Answer to RQ1: AMPLE outperforms all the baseline methods in terms of accuracy and F1 score. In particular, AMPLE achieves 7.63%, 16.48%, and 40.40% improvements in F1 score over the best baseline method on the three datasets, respectively.



(a) Average node distance

(b) Maximum node distance

Fig. 5: Average node distance (a) and maximum node distance (b) on the test set of FFMPeg+Qemu, Reveal, and Fan *et al.* The node distance is measured by the length of the shortest path between two nodes in a graph.

B. RQ2. Effectiveness of Graph Simplification

To answer the research question, we first explore the contribution of the graph simplification to the performance of AMPLE and the effectiveness of different simplification methods. We then analyze the graph simplification rate (*i.e.*, the ratio of reduced nodes and edges in code structure graphs) and the node distance (*i.e.*, average node distance and maximum node distance) in the simplified code structure graph.

1) *Impact on Model Performance:* To evaluate the contribution of the graph simplification and the effectiveness of our proposed simplification methods, we perform an ablation study on the three datasets. In particular, we compare the performance of four versions of AMPLE: without graph simplification (denoted as $Graph_{Original}$), with only TGS (denoted as $Graph_{TGS}$), with only VGS ($Graph_{VGS}$), and with both graph simplification methods ($Graph_{GS}$, the default AMPLE), with results shown in Table IV. The best result for each metric of each dataset is highlighted in bold.

Compared with $Graph_{Original}$, $Graph_{GS}$ improves the accuracy by 6.58%, 5.36%, and 6.00% on three datasets, and improves the F1 score by 12.56%, 14.20%, and 34.86% respectively. Both $Graph_{TGS}$ and $Graph_{VGS}$ outperform

TABLE IV: Effectiveness of graph simplification. “ $Graph_{Original}$ ” represents the performance of AMPLE on the original code structure graphs. “ $Graph_{TGS}$ ” and “ $Graph_{VGS}$ ” represent AMPLE’s performance on the type-based simplification strategy (TGS) and variable-based simplification strategy (VGS), respectively. “ $Graph_{GS}$ ” denotes the performance of AMPLE with both TGS and VGS.

Metrics(%) \ Dataset	FFMPeg+Qemu [17]				Reveal [20]				Fan <i>et al.</i> [29]			
	Accuracy	Precision	Recall	F1 score	Accuracy	Precision	Recall	F1 score	Accuracy	Precision	Recall	F1 score
Baseline												
$Graph_{Original}$	58.32	52.91	67.87	59.47	87.99	31.22	66.29	42.45	87.87	16.48	42.88	23.81
$Graph_{TGS}$	60.82	54.85	75.79	63.64	89.08	34.55	61.96	44.36	89.33	19.48	42.07	26.63
$Graph_{VGS}$	59.66	53.59	81.82	64.76	89.68	37.33	57.14	45.16	91.69	23.01	33.87	27.40
$Graph_{GS}$	62.16	55.64	83.99	66.94	92.71	51.06	46.15	48.48	93.14	29.98	34.58	32.11

$Graph_{Original}$ in terms of accuracy and F1 score on three datasets, which demonstrates our proposed graph simplification methods can contribute to the performance of AMPLE. In addition, $Graph_{VGS}$ slightly outperforms $Graph_{TGS}$. Compared with $Graph_{TGS}$, $Graph_{VGS}$ improves the accuracy by 0.75% and F1 score by 2.00% on three datasets on average. The results indicate that VGS contributes more to the graph representation learning than TGS.

2) *Analysis of Code Structure Graph Size*: We analyze the size of the code structure graph from two perspectives, including node distance (*i.e.* the shortest length between two reachable nodes), node and edge simplification rate (*i.e.* the ratio of reduced nodes and edges).

Node Distance: As shown in Figure 5, we count the length of the shortest path between any two reachable nodes as node distance during calculating the average node distance and maximum node distance. Due to the large computational complexity and limited resource, we only calculate the distances on the test sets for the three datasets. Compared with the original code structure graph, the average node distance and maximum node distance on three datasets drop by 41.65% and 39.68%, respectively, which indicates that our proposed simplification methods are helpful to reduce the node distance. We also notice that VGS can reduce average node distance and maximum node distance more than TGS, 30.05% *v.s.* 24.38 in terms of the average node distance. The results can explain the relatively better performance of $Graph_{VGS}$ than $Graph_{TGS}$ in vulnerability detection (as illustrated in Table IV).

Node and Edge Simplification Rate: Figure 6 shows the box-whisker plot of node and edge simplification rate on each dataset. The average simplification rate is computed by taking the average of the simplification rates for all the graphs. The overall distribution of simplification rates shows that both TGS and VGS can obviously reduce the node size and edge size of the code structure graph. With the same simplification method, the node simplification rate is higher than the edge simplification rate. Specifically, the average node simplification rate and edge simplification rate of the final simplified code structure graph on three datasets are 41.64% and 16.79%, respectively. Comparing the simplification rates of TGS and VGS, we find that TGS can reduce the code structure graph size to a greater extent, which may be attributed to that VGS only applies to

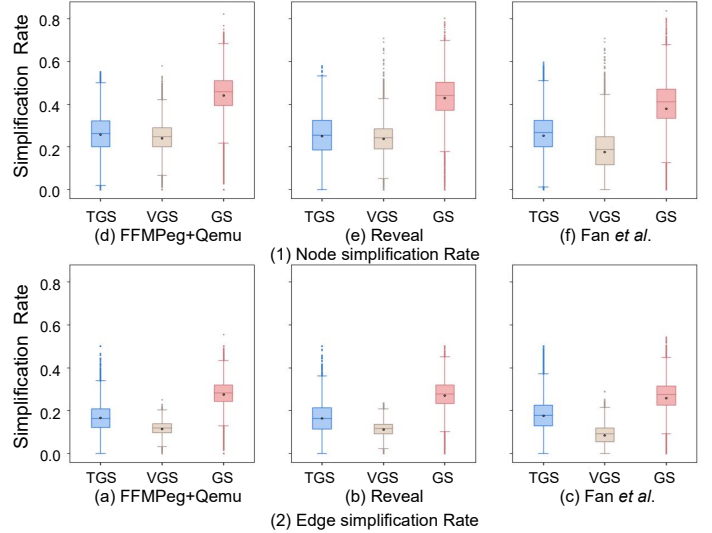


Fig. 6: Edge simplification rate and node simplification rate on three datasets.

the leaf nodes of AST.

Answer to RQ2: Graph simplification contributes significantly to the performance of AMPLE, with an F1 score improvement of 12.56%, 14.20%, and 34.86% on the three datasets, respectively. The average node, edge, and distance simplification rate is 41.64%, 16.79%, and 41.65%, respectively.

C. RQ3. Effectiveness of Enhanced Graph Representation Learning

To answer this research question, we explore the impact of the enhanced graph representation learning on AMPLE. Specifically, we study the two involved modules including the edge-aware graph convolutional network module (EA-GCN) and the kernel-scaled representation module (KSR).

1) Edge-Aware Graph Convolutional Network Module:

To explore the contribution of EA-GCN module, we create a variant of AMPLE without EA-GCN module that directly feeds the simplified code structure graph into the KSR module.

TABLE V: Impact of the EA-GCN module and the KSR module on the performance of AMPLE.

Dataset	Module	Accuracy	Precision	Recall	F1 score
FFMPeg+Qemu	w/o EA-GCN	57.13	51.60	84.53	64.08
	w/o KSR	55.89	50.90	70.65	59.17
	AMPLE	62.16	55.64	83.99	66.94
Reveal	w/o EA-GCN	85.57	27.52	57.69	37.27
	w/o KSR	79.14	20.06	60.58	30.14
	AMPLE	92.71	51.06	46.15	48.48
Fan <i>et al.</i>	w/o EA-GCN	89.79	16.73	30.48	21.60
	w/o KSR	88.97	18.37	39.62	25.10
	AMPLE	93.14	29.98	34.58	32.11

The other settings of this variant are consistent with AMPLE. As shown in Table V, EA-GCN module improves the performance of AMPLE on all datasets, *e.g.*, 4.46% in FFMPeg+Qemu, 30.08% in Reveal, and 48.66% in Fan *et al.*, in terms of the F1 score. The results indicate that the EA-GCN module focusing on the heterogeneous edge information in the graph can promote the graph representation learning and benefit the performance of vulnerability detection.

To further explore the effectiveness of the EA-GCN module, we replace the module with other existing GNN models, including GCN [54], GGNN [47], R-GCN [55] and compare them with AMPLE. As shown in Table VI, the EA-GCN module obtains significant improvements on all databases. In particular, compared to the other best performing GNN methods, the F1 score metric is improved by 6.78%, 15.48% and 39.12% on the three datasets, respectively. The EA-GCN module learns different weights for multiple types of edges, which can benefit the performance of vulnerability detection.

2) *Kernel-Scaled Representation Module*: To understand how the kernel-scaled representation module works, we also deploy a variant of AMPLE without this module. The variant directly replaces the KSR module with a fully-connected layer to classify the edge-enhanced node representation matrix learned by EA-GCN. Table V shows the performance of the variants. On all the datasets, the accuracy, F1 score and precision consistently achieve higher value with the addition of KSR module. Specially, compared with the variant without KSR module, the F1 score of AMPLE is improved by 13.13%, 57.53%, and 27.93% on FFMPeg+Qemu, Reveal, and Fan *et al.* datasets, respectively. AMPLE also increases the accuracy by 11.22%, 17.15%, and 4.69%, respectively. The results demonstrate that our proposed KSR module brings a performance improvement in vulnerability detection.

Answer to RQ3: The enhanced graph representation learning effectively improves the AMPLE performance. The EA-GCN module improves the F1 score of 4.46%, 30.08%, and 48.66% on the FFMPeg+Qemu, Reveal and Fan *et al.*, and the KSR module contributes 13.13%, 57.53%, and 27.93%, respectively.

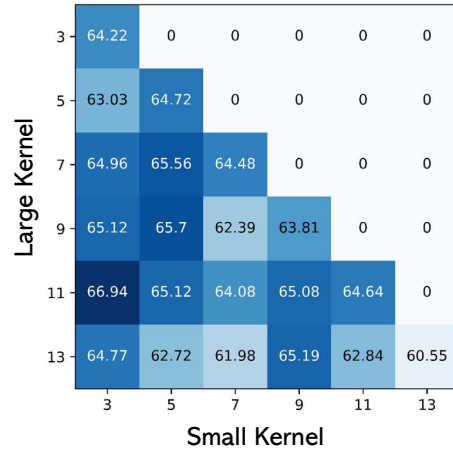


Fig. 7: Impact of kernel sizes on the F1 score of AMPLE. The x-axis and y-axis indicate the small kernel size and large kernel size, respectively. The darker the color, the better the performance.

D. RQ4: Influences of Hyper-parameters on AMPLE

To answer the research question, we explore the impact of different hyper-parameters, including the sizes of large and small convolution kernel, the layer number of EA-GCN module, and the number of the attention heads.

1) *Sizes of Large Kernel and Small Kernel*: Figure 7 shows the F1 score of AMPLE with different sizes of large kernel and small kernel. AMPLE achieves the best performance when the sizes of the large kernel and small kernel are set as 11 and 3, respectively. Two kernels of the same size bring a relatively low F1 value, which indicates that using one type of convolutional kernel does not well learn the graph representations. Besides, due to the limited number of nodes in the simplified code structure graph, the size of the large kernel cannot be increased infinitely and the F1 score starts to decrease when the kernel size equals to 13. In summary, the model benefits from a large kernel to capture the relations between distant nodes, and meanwhile retains the capability of capturing local information in the graph structure from a small kernel.

2) *Numbers of EA-GCN layers*: We also explore the effect of the number of EA-GCN layers on the performance of AMPLE. Table VII shows the results of EA-GCN with different numbers of layers on FFMPeg+Qemu dataset. As can be seen, EA-GCN with 2 layers obtains the highest accuracy of 62.16% and F1 score of 66.94%. As the number of layers continues to increase, the accuracy and F1 score decrease. We suppose that the GCN encounters an over-smoothing issue [24] with more layers and tends to learn similar embeddings for different nodes, which leads to performance degradation. AMPLE exhibits similar trends on the other datasets.

3) *Numbers of Attention Heads*: Table VII shows the performance of AMPLE with different numbers of attention heads. Generally, more heads bring a noticeable improvement

TABLE VI: Comparison between the EA-GCN module with other GNN models.

Metrics(%) \ Dataset	FFMPeg+Qemu [17]				Reveal [20]				Fan <i>et al.</i> [29]			
	Accuracy	Precision	Recall	F1 score	Accuracy	Precision	Recall	F1 score	Accuracy	Precision	Recall	F1 score
Baseline												
GGNN	55.69	50.66	78.27	61.51	89.07	34.59	52.88	41.83	90.65	18.69	30.16	23.08
GCN	60.32	54.90	68.83	61.08	88.29	32.56	53.85	40.58	88.31	14.84	31.79	20.23
R-GCN	61.40	55.70	71.67	62.69	89.14	34.81	52.88	41.98	90.29	16.70	27.14	20.67
EA-GCN	62.16	55.64	83.99	66.94	92.71	51.06	46.15	48.48	93.14	29.98	34.58	32.11

TABLE VII: The impact of the number of EA-GCN layers and attention heads on the performance of AMPLE.

layer number	Accuracy	F1 score	head number	Accuracy	F1 score
1	60.78	64.56	2	58.92	62.43
2	62.16	66.94	4	61.45	63.16
3	61.49	61.49	5	60.10	65.63
4	60.57	61.82	10	62.16	66.94
5	55.91	59.99	20	60.71	64.40

```

1 int main(int argc, char **argv) {
2   char cat[] = "cat";
3   char *command;
4   size_t commandLength;
5   commandLength = strlen(cat) + strlen(argv[1]) + 1;
6   command = (char *) malloc(commandLength);
7   strncpy(command, cat, commandLength);
8   strcat(command, argv[1], (commandLength-strlen(cat)));
9   system(command);
10  return (0);
11 }

```

Fig. 8: A heatmap of the CWE-77 [56] example correctly predicted by AMPLE. The color-shaded of a statement is drawn according to the ‘attention’ weight. Green-shaded indicates the minimum attention weight. The redder the color, the greater the ‘attention’ weight. Red colored code are vulnerable.

in accuracy and F1 score compared with fewer heads, which shows that more heads are helpful for capturing the different edge information in the code structure graph. However, employing more than 10 heads does not further improve performance.

Answer to RQ4: Different settings of hyper-parameters can influence the performance of AMPLE in vulnerability detection. Our default hyper-parameter settings achieve optimal results.

VI. DISCUSSION

A. Why Does AMPLE Work?

We identify the following two advantages of AMPLE, which can explain its effectiveness in code vulnerability detection. We also show an example of the correct prediction by AMPLE.

(1) The ability to capture global information of code structure graph. The proposed graph simplification method and kernel-scaled representation module help AMPLE learn

the global information of code structure graphs. More specifically, the proposed graph simplification methods reduce the node distance and code structure graph size, which can help AMPLE more effectively extract global information from code graphs. As shown in Figure 5, compared with the original code structure graph, the average node distance and maximum node distance on three datasets drop by 41.65% and 39.68%, respectively. Figure 6 also shows that the numbers of nodes and edges are reduced after simplification. The proposed Kernel-scaled representation (KSR) module adopts two convolution kernels with different scales: a large kernel and a small kernel. The large kernel can focus on the relations between distant nodes, which benefits the performance of AMPLE. As shown in Table V, KSR module brings obvious performance improvement to vulnerability detection, *e.g.* 32.86% in terms of F1 score on three datasets on average.

(2) The ability to handle graphs with multiple edge types.

We design the EA-GCN module for heterogeneous multi-relational code graphs. It can produce the edge-enhanced node representation matrix, which incorporates the edge information in the simplified code structure graph. As shown in Table VI, the EA-GCN module has significant advantages over all the other GNN models, with an average improvement of 2.39% and 7.40% in accuracy and F1 score, respectively.

To understand whether AMPLE pays attention to the vulnerable statements in the code, we illustrate the heatmap of attention for one example of CWE-77 [56] in Figure 8. Statements with higher attention weights are shaded in red. Following Reveal [20], we obtain the node importance by using an activation function. The activation values of each statement and its corresponding sub-AST nodes are summed as the statement’s ‘attention’ weight. Lines 8-9 are vulnerable statements and the heatmap shows that AMPLE focuses more on Line 8. Since the code in Lines 4-9 has strong semantic dependencies with Lines 8 and 9, these lines also receive relatively higher attention, which enables AMPLE to make the accurate detection (*i.e.* classifying the code as vulnerable).

In this paper, the proposed techniques benefit the graphs that contain multiple types of edges. We will investigate other types of code graphs and other tasks in our future work.

B. Threats and Limitations

The first threat to validity is about the limited number of experimental datasets. We evaluate AMPLE on three datasets: FFMPeg+Qemu, Reveal, and Fan *et al.* The main reason is that these three datasets are commonly used by previous related

work [17], [20], [21] on vulnerability detection. Although these datasets cover many different types of open source projects, we will experiment with more datasets to further evaluate the effectiveness of AMPLE in our future work.

The second threat to validity is that our proposed graph simplification is specific to C/C++ languages. We only conduct experiments on C/C++ datasets, and not on datasets of other programming languages such as Java and C#. In the future, we will select datasets in more programming languages to further evaluate our approach.

The third threat to validity is the implementation of baselines. Since Devign [17] does not publish their implementation and hyper-parameters, we reproduce Devign based on the Reveal’s [20] implementation. We try our best to tune its parameters as much as we can to achieve the similar experimental results reported in their paper.

VII. CONCLUSION

This paper proposes AMPLE, a novel vulnerability detection framework with graph simplification and enhanced graph representation learning. AMPLE can shrink the node sizes of the code structure graphs to reduce the distances between nodes. It incorporates edge types to enhance the representation of local nodes to cope with more heterogeneous multi-relations in node representations. It also can capture the knowledge of graphs by capturing the relations between distant graph nodes. Compared with state-of-the-art deep learning-based methods, AMPLE significantly improves the vulnerability detection performance on all datasets by 7.64%-199.81% with respect to the F1 score.

Data availability: Our source code as well as experimental data are available at: <https://github.com/AMPLE001/AMPLE>.

REFERENCES

- [1] “The exactis breach: 5 things you need to know.” 2000. [Online]. Available: <https://blog.infoarmor.com/individuals-and-families/the-exactis-breach-5-things-you-need-to-know>
- [2] “Wannacry ransomware attack.” 2000. [Online]. Available: https://en.wikipedia.org/wiki/WannaCry_ransomware_attack
- [3] “National vulnerability database.” 2022. [Online]. Available: <https://nvd.nist.gov/>
- [4] “Cyber security vulnerability statistics and facts of 2022.” 2022. [Online]. Available: <https://www.comparitech.com/blog/information-security/cybersecurity-vulnerability-statistics/>
- [5] “2022 open source security and risk analysis report.” 2022. [Online]. Available: <https://www.synopsys.com/software-integrity/resources/analyst-reports/open-source-security-risk-analysis.html>
- [6] S. Cherem, L. Princehouse, and R. Rugina, “Practical memory leak detection using guarded value-flow analysis,” in *Proceedings of the ACM SIGPLAN 2007 Conference on Programming Language Design and Implementation, San Diego, California, USA, June 10-13, 2007*, J. Ferrante and K. S. McKinley, Eds. ACM, 2007, pp. 480–491.
- [7] G. Fan, R. Wu, Q. Shi, X. Xiao, J. Zhou, and C. Zhang, “Smoke: scalable path-sensitive memory leak detection for millions of lines of code,” in *Proceedings of the 41st International Conference on Software Engineering, ICSE 2019, Montreal, QC, Canada, May 25-31, 2019*, J. M. Atlee, T. Bultan, and J. Whittle, Eds. IEEE / ACM, 2019, pp. 72–82.
- [8] D. L. Heine and M. S. Lam, “Static detection of leaks in polymorphic containers,” in *28th International Conference on Software Engineering (ICSE 2006), Shanghai, China, May 20-28, 2006*, L. J. Osterweil, H. D. Rombach, and M. L. Soffa, Eds. ACM, 2006, pp. 252–261.

- [9] D. Kroening and M. Tautschnig, “CBMC - C bounded model checker - (competition contribution),” in *Tools and Algorithms for the Construction and Analysis of Systems - 20th International Conference, TACAS 2014, Held as Part of the European Joint Conferences on Theory and Practice of Software, ETAPS 2014, Grenoble, France, April 5-13, 2014. Proceedings*, ser. Lecture Notes in Computer Science, E. Ábrahám and K. Havelund, Eds., vol. 8413. Springer, 2014, pp. 389–391.
- [10] X. Ji, J. Yang, J. Xu, L. Feng, and X. Li, “Interprocedural path-sensitive resource leaks detection for C programs,” in *Proceedings of the Fourth Asia-Pacific Symposium on Internetware, Internetware 2012, QingDao, China, October 30-31, 2012*, H. Mei, J. Lv, Q. Wang, and L. Liu, Eds. ACM, 2012, pp. 19:1–19:9.
- [11] Z. Li, D. Zou, S. Xu, X. Ou, H. Jin, S. Wang, Z. Deng, and Y. Zhong, “Vuldeepecker: A deep learning-based system for vulnerability detection,” in *25th Annual Network and Distributed System Security Symposium, NDSS 2018, San Diego, California, USA, February 18-21, 2018*. The Internet Society, 2018.
- [12] R. L. Russell, L. Y. Kim, L. H. Hamilton, T. Lazovich, J. Harer, O. Ozdemir, P. M. Ellingwood, and M. W. McConley, “Automated vulnerability detection in source code using deep representation learning,” in *17th IEEE International Conference on Machine Learning and Applications, ICMLA 2018, Orlando, FL, USA, December 17-20, 2018*, M. A. Wani, M. M. Kantardzic, M. S. Mouchaweh, J. Gama, and E. Lughofer, Eds. IEEE, 2018, pp. 757–762.
- [13] Z. Li, D. Zou, S. Xu, H. Jin, Y. Zhu, and Z. Chen, “Sysevr: A framework for using deep learning to detect software vulnerabilities,” *IEEE Trans. Dependable Secur. Comput.*, vol. 19, no. 4, pp. 2244–2258, 2022.
- [14] H. K. Dam, T. Tran, T. Pham, S. W. Ng, J. Grundy, and A. Ghose, “Automatic feature learning for vulnerability prediction,” *CoRR*, vol. abs/1708.02368, 2017.
- [15] Y. Wu, D. Zou, S. Dou, W. Yang, D. Xu, and H. Jin, “Vulcnn: An image-inspired scalable vulnerability detection system,” in *44th IEEE/ACM 44th International Conference on Software Engineering, ICSE 2022, Pittsburgh, PA, USA, May 25-27, 2022*. ACM, 2022, pp. 2365–2376.
- [16] F. Yamaguchi, N. Golde, D. Arp, and K. Rieck, “Modeling and discovering vulnerabilities with code property graphs,” in *2014 IEEE Symposium on Security and Privacy, SP 2014*. IEEE Computer Society, 2014, pp. 590–604.
- [17] Y. Zhou, S. Liu, J. K. Siow, X. Du, and Y. Liu, “Devign: Effective vulnerability identification by learning comprehensive program semantics via graph neural networks,” in *Advances in Neural Information Processing Systems 32: Annual Conference on Neural Information Processing Systems 2019, NeurIPS 2019, 2019*, pp. 10 197–10 207.
- [18] D. Guo, S. Ren, S. Lu, Z. Feng, D. Tang, S. Liu, L. Zhou, N. Duan, A. Svyatkovskiy, S. Fu, M. Tufano, S. K. Deng, C. B. Clement, D. Drain, N. Sundaresan, J. Yin, D. Jiang, and M. Zhou, “Graphcodebert: Pre-training code representations with data flow,” in *9th International Conference on Learning Representations, ICLR 2021, Virtual Event, Austria, May 3-7, 2021*. OpenReview.net, 2021.
- [19] X. Nguyen, S. R. Joty, S. C. H. Hoi, and R. Socher, “Tree-structured attention with hierarchical accumulation,” in *8th International Conference on Learning Representations, ICLR 2020, Addis Ababa, Ethiopia, April 26-30, 2020*. OpenReview.net, 2020.
- [20] S. Chakraborty, R. Krishna, Y. Ding, and B. Ray, “Deep learning based vulnerability detection: Are we there yet?” *CoRR*, vol. abs/2009.07235, 2020.
- [21] Y. Li, S. Wang, and T. N. Nguyen, “Vulnerability detection with fine-grained interpretations,” in *ESEC/FSE ’21: 29th ACM Joint European Software Engineering Conference and Symposium on the Foundations of Software Engineering, Athens, Greece, August 23-28, 2021*. ACM, 2021, pp. 292–303.
- [22] D. Zhu, X. Dai, and J. Chen, “Pre-train and learn: Preserving global information for graph neural networks,” *J. Comput. Sci. Technol.*, vol. 36, no. 6, pp. 1420–1430, 2021.
- [23] V. J. Hellendoorn, C. Sutton, R. Singh, P. Maniatis, and D. Bieber, “Global relational models of source code,” in *8th International Conference on Learning Representations, ICLR 2020*. OpenReview.net, 2020.
- [24] U. Alon and E. Yahav, “On the bottleneck of graph neural networks and its practical implications,” in *9th International Conference on Learning Representations, ICLR 2021, Virtual Event, Austria, May 3-7, 2021*. OpenReview.net, 2021.
- [25] Q. Li, Z. Han, and X. Wu, “Deeper insights into graph convolutional networks for semi-supervised learning,” in *Proceedings of the Thirty-*

- Second AAAI Conference on Artificial Intelligence, (AAAI-18), the 30th innovative Applications of Artificial Intelligence (IAAI-18), and the 8th AAAI Symposium on Educational Advances in Artificial Intelligence (EAAI-18), New Orleans, Louisiana, USA, February 2-7, 2018. AAAI Press, 2018, pp. 3538–3545.
- [26] H. Pei, B. Wei, K. C. Chang, Y. Lei, and B. Yang, “Geom-gcn: Geometric graph convolutional networks,” in *8th International Conference on Learning Representations, ICLR 2020, Addis Ababa, Ethiopia, April 26-30, 2020*. OpenReview.net, 2020.
- [27] F. Scarselli, M. Gori, A. C. Tsoi, M. Hagenbuchner, and G. Monfardini, “The graph neural network model,” *IEEE Trans. Neural Networks*, vol. 20, no. 1, pp. 61–80, 2009.
- [28] L. Wu, Y. Chen, K. Shen, X. Guo, H. Gao, S. Li, J. Pei, and B. Long, “Graph neural networks for natural language processing: A survey,” *CoRR*, vol. abs/2106.06090, 2021.
- [29] J. Fan, Y. Li, S. Wang, and T. N. Nguyen, “A C/C++ code vulnerability dataset with code changes and CVE summaries,” in *MSR ’20: 17th International Conference on Mining Software Repositories, Seoul, Republic of Korea, 29-30 June, 2020*. ACM, 2020, pp. 508–512.
- [30] A. Dosovitskiy, L. Beyer, A. Kolesnikov, D. Weissenborn, X. Zhai, T. Unterthiner, M. Dehghani, M. Minderer, G. Heigold, S. Gelly, J. Uszkoreit, and N. Houlsby, “An image is worth 16x16 words: Transformers for image recognition at scale,” in *9th International Conference on Learning Representations, ICLR 2021*. OpenReview.net, 2021.
- [31] S. Ioffe and C. Szegedy, “Batch normalization: Accelerating deep network training by reducing internal covariate shift,” in *Proceedings of the 32nd International Conference on Machine Learning, ICML 2015, Lille, France, 6-11 July 2015*, ser. JMLR Workshop and Conference Proceedings, F. R. Bach and D. M. Blei, Eds., vol. 37. JMLR.org, 2015, pp. 448–456.
- [32] S. Gao, C. Gao, C. Wang, J. Sun, and D. Lo, “CARBON: A counterfactual reasoning based framework for neural code comprehension debiasing,” *CoRR*, vol. abs/2207.11104, 2022.
- [33] C. Wang, Y. Yang, C. Gao, Y. Peng, H. Zhang, and M. R. Lyu, “No more fine-tuning? an experimental evaluation of prompt tuning in code intelligence,” in *Proceedings of the 30th ACM Joint European Software Engineering Conference and Symposium on the Foundations of Software Engineering, ESEC/FSE 2022, Singapore, Singapore, November 14-18, 2022*, A. Roychoudhury, C. Cadar, and M. Kim, Eds. ACM, 2022, pp. 382–394.
- [34] T. Mikolov, K. Chen, G. Corrado, and J. Dean, “Efficient estimation of word representations in vector space,” in *1st International Conference on Learning Representations, ICLR 2013, 2013*.
- [35] M. Allamanis, M. Brockschmidt, and M. Khademi, “Learning to represent programs with graphs,” in *6th International Conference on Learning Representations, ICLR 2018, Vancouver, BC, Canada, April 30 - May 3, 2018, Conference Track Proceedings*. OpenReview.net, 2018.
- [36] X. Duan, J. Wu, S. Ji, Z. Rui, T. Luo, M. Yang, and Y. Wu, “Vulsniper: Focus your attention to shoot fine-grained vulnerabilities,” in *Proceedings of the Twenty-Eighth International Joint Conference on Artificial Intelligence, IJCAI 2019*. ijcai.org, 2019, pp. 4665–4671.
- [37] Z. Song, J. Wang, S. Liu, F. Zhiyang, and K. Yang, “Hgvul: A code vulnerability detection method based on heterogeneous source-level intermediate representation,” *Security and Communication Networks*, 2022.
- [38] S. Gao, C. Gao, Y. He, J. Zeng, L. Y. Nie, and X. Xia, “Code structure guided transformer for source code summarization,” *CoRR*, vol. abs/2104.09340, 2021.
- [39] W. Ma, M. Zhao, E. O. Soremekun, Q. Hu, J. M. Zhang, M. Papadakis, M. Cordy, X. Xie, and Y. L. Traon, “Graphcode2vec: Generic code embedding via lexical and program dependence analyses,” in *19th IEEE/ACM International Conference on Mining Software Repositories, MSR 2022, Pittsburgh, PA, USA, May 23-24, 2022*. ACM, pp. 524–536.
- [40] A. Krizhevsky, I. Sutskever, and G. E. Hinton, “Imagenet classification with deep convolutional neural networks,” in *Advances in Neural Information Processing Systems 25: 26th Annual Conference on Neural Information Processing Systems 2012. Proceedings of a meeting held December 3-6, 2012, Lake Tahoe, Nevada, United States*, P. L. Bartlett, F. C. N. Pereira, C. J. C. Burges, L. Bottou, and K. Q. Weinberger, Eds., 2012, pp. 1106–1114.
- [41] Y. LeCun, L. Bottou, Y. Bengio, and P. Haffner, “Gradient-based learning applied to document recognition,” *Proc. IEEE*, vol. 86, no. 11, pp. 2278–2324, 1998.
- [42] S. O. Alhumoud and A. A. A. Wazrah, “Arabic sentiment analysis using recurrent neural networks: a review,” *Artif. Intell. Rev.*, vol. 55, no. 1, pp. 707–748, 2022.
- [43] T. Mikolov and G. Zweig, “Context dependent recurrent neural network language model,” in *2012 IEEE Spoken Language Technology Workshop (SLT), Miami, FL, USA, December 2-5, 2012*. IEEE, 2012, pp. 234–239.
- [44] X. Gong, Z. Xing, X. Li, Z. Feng, and Z. Han, “Joint prediction of multiple vulnerability characteristics through multi-task learning,” in *24th International Conference on Engineering of Complex Computer Systems, ICECCS 2019*. IEEE, 2019, pp. 31–40.
- [45] M. Gori, G. Monfardini, and F. Scarselli, “A new model for learning in graph domains,” in *Proceedings. 2005 IEEE International Joint Conference on Neural Networks, 2005.*, vol. 2, 2005, pp. 729–734 vol. 2.
- [46] F. Scarselli, M. Gori, A. C. Tsoi, M. Hagenbuchner, and G. Monfardini, “The graph neural network model,” *IEEE Trans. Neural Networks*, vol. 20, no. 1, pp. 61–80, 2009.
- [47] Y. Li, D. Tarlow, M. Brockschmidt, and R. S. Zemel, “Gated graph sequence neural networks,” in *4th International Conference on Learning Representations, ICLR 2016, 2016*.
- [48] S. Cao, X. Sun, L. Bo, R. Wu, B. Li, and C. Tao, “MVD: memory-related vulnerability detection based on flow-sensitive graph neural networks,” *CoRR*, vol. abs/2203.02660, 2022.
- [49] M. Fu and C. Tantithamthavorn, “Linevul: A transformer-based line-level vulnerability prediction,” 2022.
- [50] F. Yamaguchi, N. Golde, D. Arp, and K. Rieck, “Modeling and discovering vulnerabilities with code property graphs,” in *2014 IEEE Symposium on Security and Privacy, SP 2014*. IEEE Computer Society, 2014, pp. 590–604.
- [51] Y. Wang and H. Li, “Code completion by modeling flattened abstract syntax trees as graphs,” in *Thirty-Fifth AAAI Conference on Artificial Intelligence, AAAI 2021, Thirty-Third Conference on Innovative Applications of Artificial Intelligence, IAAI 2021, The Eleventh Symposium on Educational Advances in Artificial Intelligence, EAAI 2021, Virtual Event, February 2-9, 2021*. AAAI Press, 2021, pp. 14015–14023.
- [52] A. Vaswani, N. Shazeer, N. Parmar, J. Uszkoreit, L. Jones, A. N. Gomez, L. Kaiser, and I. Polosukhin, “Attention is all you need,” in *Advances in Neural Information Processing Systems 30: Annual Conference on Neural Information Processing Systems 2017, December 4-9, 2017, Long Beach, CA, USA*, I. Guyon, U. von Luxburg, S. Bengio, H. M. Wallach, R. Fergus, S. V. N. Vishwanathan, and R. Garnett, Eds., 2017, pp. 5998–6008.
- [53] L. Liu, H. Jiang, P. He, W. Chen, X. Liu, J. Gao, and J. Han, “On the variance of the adaptive learning rate and beyond,” in *8th International Conference on Learning Representations, ICLR 2020*. OpenReview.net, 2020.
- [54] T. N. Kipf and M. Welling, “Semi-supervised classification with graph convolutional networks,” in *5th International Conference on Learning Representations, ICLR 2017, Toulon, France, April 24-26, 2017, Conference Track Proceedings*. OpenReview.net, 2017.
- [55] M. S. Schlichtkrull, T. N. Kipf, P. Bloem, R. van den Berg, I. Titov, and M. Welling, “Modeling relational data with graph convolutional networks,” in *The Semantic Web - 15th International Conference, ESWC 2018*, ser. Lecture Notes in Computer Science, vol. 10843. Springer, 2018, pp. 593–607.
- [56] “Cwe-77.” [Online]. Available: <https://cwe.mitre.org/data/definitions/77.html>